



Title	Study of the Welding Process for Improving the Deformation Capacity of the Beam-to-column Joint
Author(s)	Kasai, Ryu; Suzuki, Reiichi; Suga, Tetsuo et al.
Citation	Transactions of JWRI. 2015, 44(1), p. 1-8
Version Type	VoR
URL	<a href="https://doi.org/10.18910/57266">https://doi.org/10.18910/57266</a>
rights	
Note	

*The University of Osaka Institutional Knowledge Archive : OUKA*

<https://ir.library.osaka-u.ac.jp/>

The University of Osaka

# Study of the Welding Process for Improving the Deformation Capacity of the Beam-to-column Joint<sup>†</sup>

KASAI Ryu\*, SUZUKI Reiichi\*\*, SUGA Tetsuo\*\*\* and NAKAGOMI Tadao\*\*\*\*

## Abstract

*In order to improve the seismic resistance of the beam-to-column joint, the authors have studied the welding procedures that can reduce the stress concentration induced by steel backing and scallop toe, maintaining the merits of the on-site welding without bracket. Consequently, it has been found that the seismic resistance of the joint can be improved by employing the backing-less process that replaces the steel backing with the overhead MAG weld made using a special flux-cored wire and by applying the reinforcement buildup welding at the scallop toe by MAG welding with a conventional solid wire.*

**KEY WORDS:** (Column-to-beam joint), (MAG welding), (Non-steel-backing), (Backing metal), (Flux-cored wire), (Overhead position), (Overlaying), (Seismic resistance)

## 1. Introduction

Recently, there have been many cases where the column and beam components are erected by on-site welding in the construction of steel frames with the column-beam connection without bracket. This is intended to cut construction costs by simplifying the construction process, make the vehicle-mounted transportation more efficient, and reduce the emission of CO<sub>2</sub> with improved transportation efficiency. However, with this structural type, the column-beam connection cannot be turned over and hence requires the steel backing attached on the outside of the bottom flange of the beam, which results in a vertically asymmetric weld joint configuration as shown in **Fig. 1**. It has been pointed out that when the column-beam joint is loaded with the amplitude stress caused for instance by an earthquake, a large amount of tensile stress can be generated in the outside of both top and bottom flanges due to the characteristic of H-beam steel structure, and in turn the steel backing area in the outside of the bottom flange carries a high degree of stress concentration due to the notch effect of the base metal-steel backing opening, thereby causing the initiation of brittle fracture.<sup>1)</sup>

In order to solve the above-mentioned problem, the authors have studied to develop the welding procedures that can reduce the stress concentration in the steel backing areas, maintaining the merits of the erection by

on-site welding. In this study, the reinforcement method has also been examined to reduce the stress concentration in the junction of scallop and bottom flange (so-called scallop toe) which is known as another stress raiser in the column-beam joint.

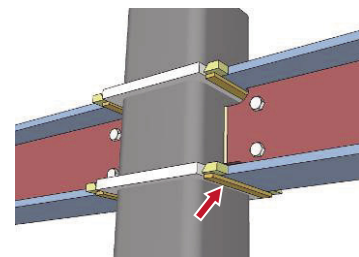


**Fig. 1** Schematic diagram of the beam-to-column joint

## 2. Development of the backing-less process (without steel backing)

### 2.1 Development goal for backing-less process

The backing-less process by overhead welding was examined to replace the steel backing, thereby reducing the stress concentration. More specifically, this study has targeted the development of the overhead-flat combined welding process that uses a highly efficient welding consumable dedicated to overhead welding to build up

<sup>†</sup> Received on June 1, 2015

\* Shinko Welding Service Co., Ltd.

\*\* Kobe Steel, Ltd.

\*\*\* Visiting Professor

\*\*\*\* Waseda Univ.

## Study of the Welding Process for Improving the Deformation Capacity of the Beam-to-column Joint

the weld layers without a steel backing, followed by ordinary flat welding to fill the groove on the other side.

In the overhead-flat combined welding process, the following performances are desired for the overhead melt-through weld: (1) stable overhead welding, (2) sufficient throat thickness to prevent excessive melt-through by the first filling pass laid afterward in the flat position without a steel backing, and (3) easily obtainable good-wash flat bead without convex irregularity to reduce the stress concentration in order for seismic stresses to be transferred smoothly in the column-beam areas.

### 2.2 Problems with conventional wires and development of dedicated overhead welding wire

Generally, the welding consumables for welding the column-beam connections are the solid wires of YGW11 and YGW18 specified by JIS Z 3312. However, if such standard wires are used in overhead melt-through welding, the following problems may occur: (1) the arc force is too strong to form an adequate melt-through weld; (2) the use of a lower current to weaken the arc force causes an unstable arc; (3) a large amount of coarse particle spatter falls toward the welder; and (4) the molten metal is prone to sag causing a convex bead due to slower solidification rates. This is why the welders are required to possess high skills and take safety measures; in addition, they are obliged to carry out frequent incidental repair work such as grinding in the overhead position, and thus they will avoid overhead welding. With conventional backing-less processes, it was not attempted to improve such problems.

Taking this into consideration, an appropriate overhead welding process was examined to overcome the (1)-(4) problems. Consequently, the special flux-cored wire of basic type was newly developed (referred to as "developed FCW" hereinafter)<sup>2)</sup>, which corresponds to T49J0T5-1CA-U per JIS Z 3313. The developed FCW was designed to use the extraordinary electric wire connection of direct-current electrode-negative polarity (wire: minus; base metal: plus), reversal to that used in conventional MAG welding, in order to exert its best performance for the present particular application.

This new welding process excels in the performances as discussed below. Firstly, it features low spatter with fine particles because (1) the basic chemical compound (barium fluoride) contained in the cored flux vaporizes in the arc to generate the high vapor pressure acting against the arc force; and (2) the DCEN polarity causes the cation to impact the molten wire tip. The (1) and (2) forces impact in the molten droplet on the wire tip to separate it into smaller particles of molten droplets, thereby creating a spray droplet transfer. The excellent overhead welding performance of the new process can be attributed to the effect of the deoxidizers appropriately dosed in the developed FCW, which increases the surface tension of the weld pool, and to the lower welding efficiency (the deposition rate per amperage). Due to these two characteristics, the weld metal becomes hard to sag. The

new process excels in depositing a flat bead because the fine grains of molten droplets are distributed in a wider area by the spray arc.

**Table 1** shows the mechanical and chemical properties of the deposited metal of the developed FCW in comparison with those of a standard wire of JIS Z 3312 YGW11. From these data, it can be confirmed that the deposited metal has the sufficient properties for the standard steel materials of SN400A~C and SN490A~C specified in JIS G 3136 that are used generally for beam and flange materials. **Table 2** shows the summary of the characteristic performances of the developed FCW for overhead welding in comparison with commonly used solid wire and conventional FCW. From the data shown in Table 2, it can be found that the developed FCW features low spatter and flat bead shape as compared with the other wires.

**Table 1** Mechanical and chemical properties of deposited metal

	Tensile test			Impact test		
	YP (MPa)	TS (MPa)	EL. (%)	vE <sub>0</sub> (J)		
Dev. FCW	458	582	30	119		
YGW11	490	570	28	120		
	Chemical composition (mass%)					
	C	Si	Mn	P	S	Al
Dev. FCW	0.12	0.15	1.14	0.015	0.005	1.0
YGW11	0.08	0.51	1.10	0.010	0.010	—

**Table 2** Performances of developed FCW vs. conv. wire

	Dev. FCW	Conv. solid wire	Conv. FCW
JIS standard	Z 3313 T49J0T5-1CA-U	Z 3312 YGW11, YGW18, etc.	Z 3313 T49J0T1-1CA-U, etc.
Polarity	DCEN	DCEP	
Wire dia.	1.4 mm	1.2 mm, 1.4 mm	
Shielding gas	CO <sub>2</sub>		
Spatter qty at low amp.	Little	Much	Much
Deposition efficiency	Low	High	Slightly high
Sagging tendency	Hard	Easy	Slightly hard
Overhead welded bead shape	Flat	Convex	Slightly convex
Penetration	Shallow	Deep	Slightly deep

A welding test was conducted in the groove with a taper gap to confirm the tolerability to the variable root gap; as a result, the tolerable greatest root gap with the new welding process has been clarified to be as large as slightly over 7 mm, which is a sufficient root gap

tolerance to overcome the practical root gap range observed in the actual erection sites

**2.3 Optimization of layer details**

Not only the one-pass welding procedure reported in the past <sup>3),4)</sup>, but also several two-pass procedures were examined. This was to ensure the good overhead weldability as well as the adequate throat thickness for the prevention of excessive melt-through when highly efficient flat welding is applied afterward from the other side and to deposit the flat bead with less stress concentration for improving the fatigue strength as compared with the steel backing process. The root gap was set to be 5 mm with the testing steel plate of SN490B, and the weld pass sequences shown in **Fig. 2** were examined. These pass sequences can be detailed as follows: (a) conventional one-pass welding procedure; (b) 1-layer-2-pass welding procedure aiming to improve bridgeability and weld toe shape; (c) 1-layer-2-pass welding procedure with the purpose of ensuring bridgeability and throat thickness; and (d) 2-layer-2-pass welding procedure intending to ensure bridgeability, throat thickness, and better bead contour. The leg length of the weld was aimed to be 11 mm. For each welding procedure, evaluated was the ease of welding operation and the macro-sectional bead shape. The level of welding difficulty was judged whether special torch manipulation was necessary or not to control the weld pool for sufficient bridging and better bead shape. The welding conditions are shown in **Table 3**.

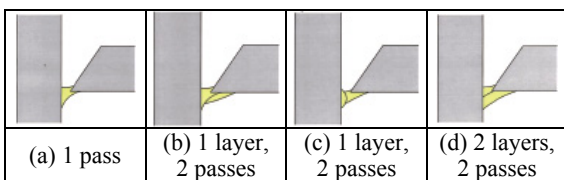


**Fig. 2** Overhead welding pass sequences (Root gap: 5 mm)

**Table 3** Welding conditions

Welding wire	Developed FCW, JIS Z 3313 T 49J0T5-1CA-U, 1.4 mmφ
Current polarity	DCEN
Current	130~150 A
Voltage	18~19 V
Wire extension	15~20 mm
Shielding gas	100%CO <sub>2</sub> , 25 L/min

Individual cross-sectional macrographs of welds are shown in **Fig. 3**. Although the conventional one-pass welding procedure enabled filling the root, it required the elaborate welding conditions to deposit a large leg length weld to fulfill root-gap bridgeability, sufficient throat thickness and leg length at the same time; hence, considerably high welding skill was required to control the torch manipulation (Fig. 3(a)). In comparison with the one-pass welding procedure, the 1-layer-2-pass welding

procedures were somewhat easier to apply: however, the bead-to-bead lapped area was apt to become concave with a thin throat, and hence these procedures are not suitable for the present study purposes of preventing excessive melt-through in the subsequent flat welding and of ensuring seismic resistance as well as fatigue strength (Fig. 3(b) (c)). It can be presumed that these problems will not be solved even if the leg length of the second pass would be changed.

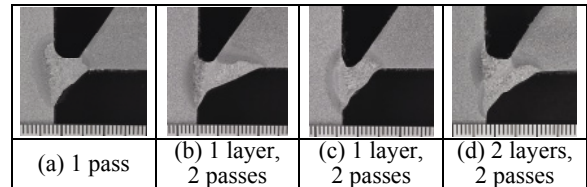


**Fig. 3** Cross-sectional macrographs  
(Refer to the pass sequences shown in Fig. 2)

By contrast, with the 2-layer-2-pass welding procedure, bridging the root could be executed by the first pass, and in the second pass the welder could concentrate on laying a large-leg weld bead to ensure sufficient throat and leg length; hence, this procedure was remarkably easy to apply without a high skill (Fig. 3(d)). In addition, the time for welding was 25-50% less than with the 1-pass welding procedure; thus, the operation was easier for the welder due to less burden and stress. The throat thickness was enough to prevent excessive melt-through in the subsequent flat welding on the other side at a high current of about 250-300A to be used in the erection on-site welding. The cross-sectional macrograph of the actual groove weld shown in **Fig. 4** clarifies that the overhead weld throat is sufficient to accommodate the penetration depth of the first pass in the flat welding. The weld toe on the flange side, which is generally deemed critical to crack initiation, exhibits a flat contour with a good wash on the base metal in the use of the developed welding process; hence it can be assumed that the stress concentration at the weld toe may be reduced and thus become advantageous in the fatigue strength and the resistance against seismic brittle fracture. The authors determined to employ the 2-layer-2-pass welding procedure for the developed welding process.

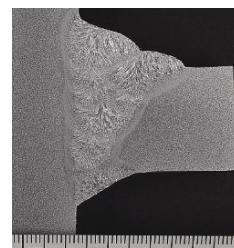


**Fig. 4** Cross-sectional macrograph by overhead-flat combined welding (Overhead welding: 2 layers, 2 passes)

## Study of the Welding Process for Improving the Deformation Capacity of the Beam-to-column Joint

### 2.4 Weld joint characteristics by backing-less process

To investigate the characteristics of the weld joint made by the backing-less process, a cruciform weld joint was assembled with a 25-mm thick steel plate of SN490B. For the weld metal, tensile test, impact test, and Vickers hardness test were carried out. For the weld joint, a cruciform joint tensile test was conducted in accordance with the Supplementary Provision 3 (Qualification Test of Electroslag Welding) of JASS6<sup>5)</sup>. The welding conditions are shown in Fig. 5 and Table 4.

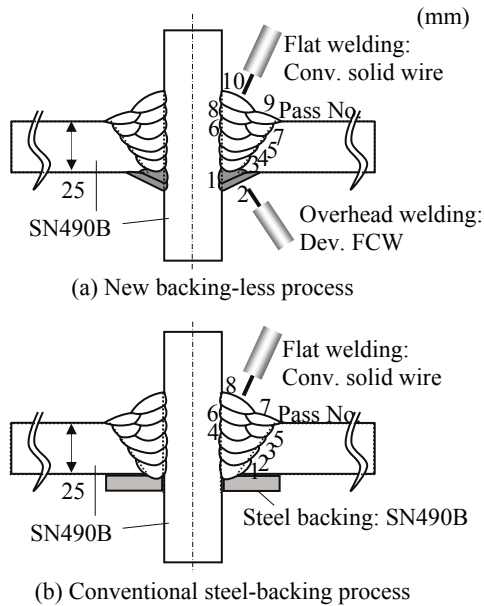


Fig. 5 Pass sequences for cruciform weld joints

Table 4 Welding conditions for cruciform joint

	Backside welding (New process only)	Surface side welding
Welding wire	JIS Z 3313 T49J0T5-1CA-U	JIS Z 3312 YGW11
Wire dia.	1.4 mmφ	1.2 mmφ
Polarity	DCEN	DCEP
Current	130~150 A	260~280 A
Voltage	18~19 V	31~34 V
Wire extension	15~20 mm	20 mm
Heat input	30 kJ/cm max.	
Interpass temp.	250°C max.	
Welding position	Overhead	Flat
Pass sequence	2 layers, 2 passes	8 passes
Shielding gas	100%CO <sub>2</sub> , 25 L/min	

The test results are shown in Table 5. The results of both tension and impact tests satisfied the standard values for SN490B steel material (tensile strength: 490 MPa min.; proof strength: 325 MPa min.; elongation: 21% min.; Charpy absorbed energy: vE<sub>0</sub> 27J min.). For the hardness distribution, the new process resulted in a maximum hardness of 248 HV, comparable to a

maximum hardness of 243 HV with the conventional steel-backing process. In the cruciform joint tension test, the test specimens fractured at the base metal zone for both the new process and the conventional steel-backing process. From these data, it has been confirmed that the new process can provide the weld joint properties comparable to those with the conventional steel-backing process, satisfying the fundamental mechanical properties required for the weld joint.

Table 5 Mechanical properties of weld metal and joint

	Tensile test of weld metal			Impact test
	YP (MPa)	TS (MPa)	El. (%)	vE <sub>0</sub> (J)
New process	542	617	29	58
Steel-backing process	541	620	29	81

	Tensile test of cruciform weld joint		
	TS (MPa)	Fracture location	Fractured specimen
New process	581	Base metal	
Steel-backing process	586	Base metal	

### 2.5 Verification test of cruciform joint fatigue strength

For evaluating the characteristics of the weld joint made by the backing-less process, the authors have focused on the fatigue strength, which can most strongly be affected by the stress concentration, and conducted the three-point bending fatigue test with the cruciform weld joints stated in the previous section. Fatigue testing was carried out under the load conditions with a stress ratio of 0.1, a frequency of 15 Hz, and a support-to-support distance of 150 mm. The stress calculation was conducted based on the stress at the center of the supports. This was because the relative comparison between the conventional steel-backing process and the new backing-less process was important and there was no remarkable difference as to the distance between the center of the supports and the crack initiation point for the two processes. More specifically, the stress calculation was executed by the following formula:  $(3 \times \text{test load} \times \text{support-to-support distance}) / (2 \times \text{plate width} \times \text{square of plate thickness})$ . For calculating the bending moment the following formula may be used:  $(\text{one-end-support reactive force}) \times (\text{length to the plate surface at the specimen center})$ . However, because the relative comparison between the conventional process and the new process was the key point, and the bending moment about any of the moment-arm applying points

along the plate thickness-wise center at the specimen center was not varied, the abovementioned formula was used. The results are summarized in the S-N diagram shown in Fig. 6.

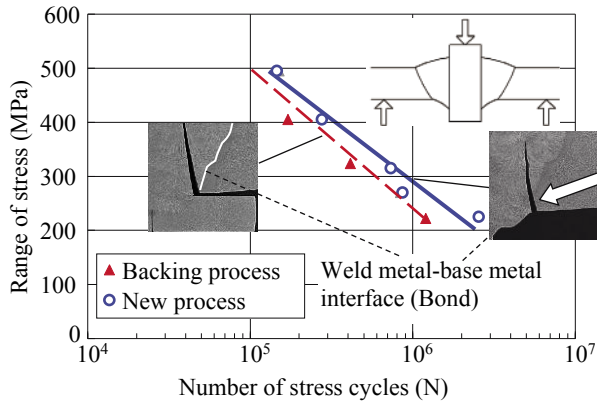


Fig. 6 Fatigue test results

The fatigue test results have clarified that with the conventional steel-backing process, the fatigue cracking was initiated from the slit between the steel backing and the beam flange, whereas with the backing-less process, it was started from the backside weld toe on the beam side. It has been revealed that the fatigue strength with the new backing-less process is superior to that with the conventional steel-backing process. Several factors, specifically the following two main factors multiplied, can be cited as to the reasons for superior fatigue strength with the new backing-less process.

(1) Effect of dimensional improvement: The new process does not require the steel backing, which inevitably causes the stress concentration due to the beam-to-steel backing discontinuity, and reduces the stress concentration degree because the backside weld toe features a smooth shape with a good wash.

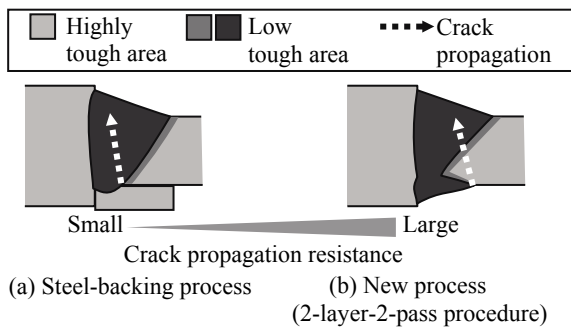


Fig. 7 Principle of microstructural improvement by new process

(2) Effect of microstructural improvement: As shown schematically in Fig. 7, the backside weld toe, which may be a crack initiation site, is away from the fusion line of the flat groove weld. Hence, even if a crack occurs, its

initiation and propagation locations will not exist in the weld metal or fusion line, which is apt to be brittle-fractured in nature, but in the heat-unaffected base metal whose crack propagation resistance is high.

### 3. Development of the reinforcement buildup welding process for scallop toe

In addition to the steel backing, scallop toe is another site where stress concentration may be induced in the column-to-beam joint; i.e., if its geometrical nature can be improved, a remarkable increase in the fatigue strength of the joint can be expected. In the on-site welding of the column-beam connection, unlike in the factory welding, the connection cannot be turned over. Hence, when a H-shape steel frame is used for the beam, scallop is required in the web on the bottom flange side in order to obtain a sound groove weld by highly efficient flat welding. Following to the backing-less process discussed above, the authors examined the reinforcement process by buildup welding of the scallop toe area. In this examination, targeted were the following effects: (1) dispersion of the deformation load that tends to concentrate in conventional scallop toe; (2) an increase in the thickness and rigidity of the flange in contact with scallop; and (3) an increase in the cross-sectional strength by placing the tip of the buildup weld metal on the diaphragm or the beam-end weld metal that is thicker than the flange thickness.<sup>6,7)</sup>

Specifically, subsequent to the complete joint penetration welding of the single bevel groove at the beam end, the reinforcement buildup welding was carried out with an appropriate length of the multi-layer fillet weld laid around the scallop toe as shown in Fig. 8 and Fig. 9. With the same welding wire of YGW11 with a diameter of 1.2 mm as used in the groove welding, the reinforcement buildup welding was carried out on three locations one by one: beneath the scallop, web's right side, and web's left side.

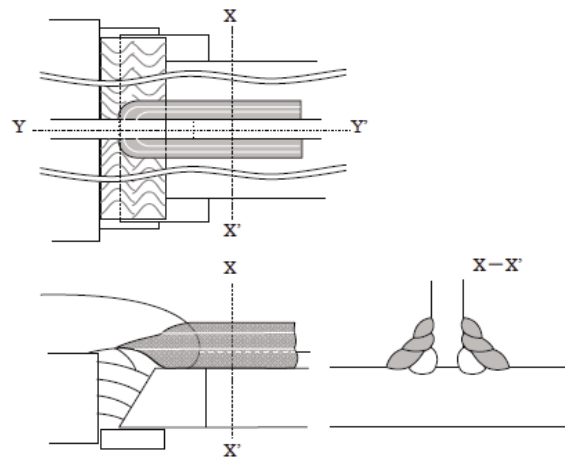


Fig. 8 Image of the reinforcement welding method around scallop toe

# Study of the Welding Process for Improving the Deformation Capacity of the Beam-to-column Joint

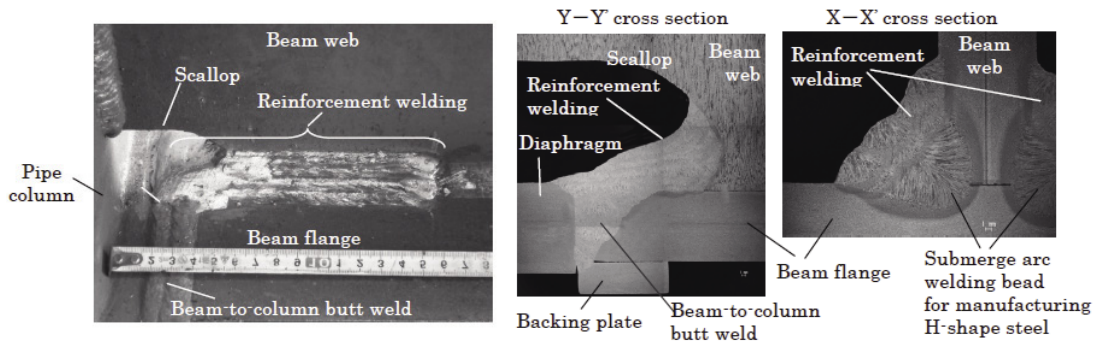


Fig. 9 Bead appearance and cross sectional bead shape of the reinforcement welding

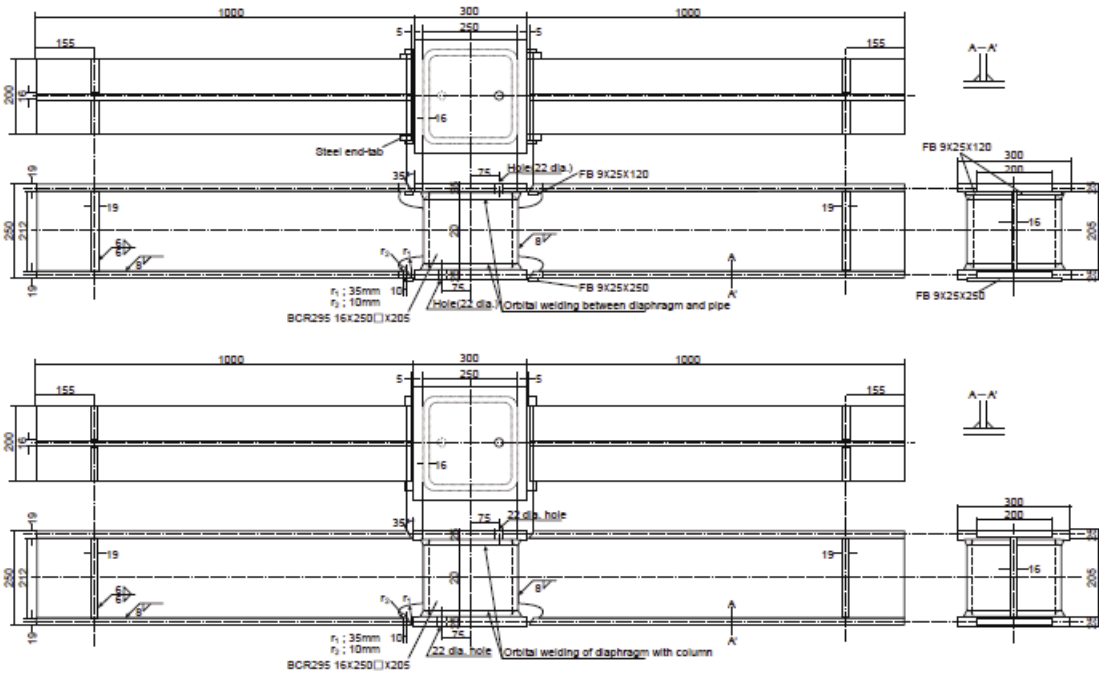


Fig. 10 Schematic diagrams of full size beam-column assemblies (Upper: conventional; Lower: developed method )

Table 6 Test models for plastic deformation test

Test No.	Type	Upper flange		Lower flange		
		Scallop	Back	Scallop	Leg length mm	Back
A	Conventional	Scallop	Steel plate	Scallop	-	Steel plate
B	Reinforcement	None	Steel plate	Scallop	10	Steel plate
C				+	15	
D				Reinfmt	20	
E	Reinfmt + backing-less		Backing-less		20	Backing-less

## 4. Verification test of deformation capacity

### 4.1 Shape of testing weld assembly

For verifying the effects of the backing-less process and the reinforcement buildup welding process for scallop toe, the mock-up test assemblies as shown in Fig. 10 were prepared and tested under repetitive loads. All the materials for diaphragm, beam flange, and beam web were of SN490B. Five testing assemblies in total were prepared as shown in Table 6. The testing parameters

were the presence or absence of steel backing and reinforcement buildup weld as well as the leg length of buildup weld. For all the testing assemblies, the upper flange joints were prepared without scallop except for the conventional on-site model of No. A for comparison, whereas the lower flange joints were assembled with the scallop as per the JASS6 standard. The reinforcement buildup weld was controlled so that (1) it extended from scallop toe to the edge of the groove weld on the column

side; (2) it reached a length of 100 mm towards the opposite side of the column; and (3) its lower leg length was set to be 16 mm with variable upper leg lengths on the web side. That is, the upper leg length (web-side leg length) was set to be 10 mm (No. B), 15 mm (No. C), and 20 mm (No. D), respectively. In addition, for the test assembly (No. E) made by the backing-less process, the upper leg length was set to be 20 mm.

**4.2 Method of repetitive loading test**

With the mock-up test assemblies of column-beam structure prepared in the previous conditions, the plastic deformation capacity was measured, in consideration of earthquake, through the repetitive loading test of the 3-point bending mode. More specifically, a 2000-kN universal testing machine was used to apply a vertical load at the central column portion of the testing assembly supported at both ends. The repetitive load was directed towards the plus and minus sides alternately with a gradually increased load amplitude,  $1c\delta p$ ,  $2c\delta p$ ,  $4c\delta p$ ,  $6c\delta p$ , and so on, based on the deformation displacement of  $c\delta p$  at the beam ends associated with the fully plastic moment of the beam component. At each amplitude except  $1c\delta p$ , two cycles of loading were repeated until the beam flange fractured. During the test, the temperature of the testing zone was kept at 0°C by using dry ice and alcohol. The deformation capacity was evaluated with the cumulative plastic deformation ratio  $\eta_s$  that was obtained with the plastic energy  $W_s$  (absorbed in the skeleton curve corresponding to the load range over the maximum proof strength of the steel material) divided by the full-plastic proof strength and strain at the beam end.

**4.3 Test results and discussions**

Table 7 shows the test results of load-strain curve, fracture pass, and the deformation ratio  $\eta_s$ . For the conventional on-site welding type of No. A, the cracking was centered in the scallop toe on the lower flange side, which propagated towards the beam flange width, and thus the deformation capacity was minimal with the lowest  $\eta_s$  of 2.6.

By contrast, for the testing assembly with reinforcement buildup weld, the fracture was centered at the buildup weld toe and propagated to the slits between the beam flange and bilateral steel tabs, reaching the interior of the beam-end weld metal and the weld metal-beam flange interface.

For the testing assemblies of No. B-D, the deformation capacity was improved with an increase in the upper leg length of the buildup weld from 10 to 15 and 20 mm. The main mechanism of improving the plastic deformation capacity in the use of the reinforcement buildup welding process for scallop toe can be presumed such that the buildup weld changed the shape of the scallop toe area to disperse the stress to be concentrated at the conventional scallop toe.

The testing assembly of No. E was prepared by the reinforcement buildup welding process for scallop toe in conjunction with the backing-less process; hence, no steel

backing was involved in the crack propagation and thus the effects of the presence and absence of steel backing could not be tested. Anyhow, the cumulative plastic deformation ratio  $\eta_s$  resulted in the highest value of 10.3. The highest plastic deformation capacity should not simply be attributed to the matter of stress concentration level associated with the presence or absence of steel backing; i.e., the strain balance in the flange's edge face and web area (flange's widthwise center area) should also be considered for another reason. Such details will be examined through further experiments and FEM analysis in the future.

**Table 7** Results of plastic deformation test

Test No.	Load-strain curve	Fracture pass	$\eta_s$
A		Lower flange under the toe of scallop	2.6
B		Connecting line of slit between the steel tab and lower flange at both sides and toe of reinforcement weld at center	5.2
C		Connecting line of slit between the steel tab and lower flange at both sides and toe of reinforcement eld at center	6.5
D		Connecting line of slit between the steel tab and lower flange at both sides and toe of reinforcement weld at center	7.2
E		Connecting line of slit between the steel tab and lower flange at both sides and toe of reinforcement weld at center	10.3

## Study of the Welding Process for Improving the Deformation Capacity of the Beam-to-column Joint

### 5. Conclusions

As discussed in the present report, the authors have developed the backing-less welding process and the reinforcement buildup welding process in order to improve the seismic resistance of the beam-to-column joint, maintaining the merits of on-site welding without bracket.

- 1) The backing-less process can be characterized by the overhead welding on the bottom flange of the column-to-beam connection without a steel backing. This process uses the dedicated welding wire which features excellent overhead welding performance for depositing a 2-layer-2-pass weld. With this new process, (1) the stress concentration can be reduced with a good-wash bead shape without a steel backing; and (2) the crack initiation site can be positioned in the highly tough heat-unaffected base metal.
- 2) The reinforcement buildup welding process can strengthen the scallop toe which exists inevitably in the web component on the bottom flange side. This process can also be applied, as a seismic strengthening process, to the building constructions completed already. The reinforcement by buildup welding probably improves the rigidity of the weld joint and the stress balance across the beam width.

It has also been suggested that the combined use of the previous two processes can improve the seismic resistance of the joint. In order to clarify the improvement mechanism, the authors will cumulate the test data to upgrade the experimental reliability and employ the FEM analysis in the future.

### References

- [1] Y. Matsumoto: Field welding problems with beam end joints, *Journal of Architecture and Building Science*, 125(2010), 39.(in Japanese)
- [2] T. Kurokawa, F. Koshiishi, H. Uchiyama, I. Aida, and T. Suga: Patent No.3586362, *Patent Journal* (2004), 1-11.(in Japanese)
- [3] M. Sato: The latest trend of welding consumables, *Welding Technique*, 48-5(2000), 58-64.(in Japanese)
- [4] A. Yamamoto and F. Koshiishi: Welding process for seismic resistant steel column-beam joints by using the new slag-type flux-cored wire "DW-1ST," *Kobe Steel Engineering Reports*, 50-1(2000), 76.(in Japanese)
- [5] Architectural Institute of Japan: *Japanese Architectural Standard Specification, JASS6, Steel-frame work* (2007), 76-78. (in Japanese)
- [6] R. Kasai et al. : Improvement of the deformation capacity of the column-to-beam joint by the reinforce welding method around the scallop bottom (No.1 method), *Summaries of Technical Papers of Annual Meeting, Architectural Institute of Japan* (2013), No.1587. (in Japanese)
- [7] R. Suzuki et al. : Improvement of the deformation capacity of the column-to-beam joint by the reinforce welding method around the scallop bottom, *Prep. Nat. Meet. JWS*, Vol.93, No.402, Autumn, 2013. (in Japanese)